



Grant Agreement No: 101004761

# AIDAinnova

Advancement and Innovation for Detectors at Accelerators  
Horizon 2020 Research Infrastructures project AIDAINNOVA

## MILESTONE REPORT

# PRODUCTION OF DLC WITH ION BEAM DEPOSITION AND PULSED LASER DEPOSITION

## MILESTONE: MS26

---

**Document identifier:**

**Due date of milestone:** End of Month 23 (February 2023)

**Report release date:** 28/02/2023

**Work package:** WP7: Gaseous Detectors

**Lead beneficiary:** INFN

**Document status:** Final

---

### Abstract:

Diamond-Like Carbon (DLC) resistive layers are a key ingredient for increasing the rate capabilities of Micro-Pattern Gaseous Detectors (MPGDs). Their production method and related quality is studied by ion beam deposition and pulsed laser deposition. The current DLC sample size will be scaled up gradually to  $10 \times 10 \text{ cm}^2$ , their quality is assessed for the production of detector-grade amplification structures.

AIDAinnova Consortium, 2023

For more information on AIDAinnova, its partners and contributors please see <http://aidainnova.web.cern.ch/>

The Advancement and Innovation for Detectors at Accelerators (AIDAinnova) project has received funding from the European Union's Horizon 2020 Research and Innovation programme under Grant Agreement no. 101004761. AIDAinnova began in April 2021 and will run for 4 years.

### Delivery Slip

	Name	Partner	Date
<b>Authored by</b>	A.P. Caricato A. Valentini P.Verwilligen	INFN INFN INFN	17/02/2023
<b>Edited by</b>	P. Verwilligen [Task coordinator]	INFN	24/02/2023
<b>Reviewed by</b>	S. Dalla Torre B. Schmidt [WP coordinator] Paolo Giacomelli [Scientific coordinator]	INFN CERN INFN	24/02/2023
<b>Approved by</b>	Paolo Giacomelli [Scientific coordinator] Steering Committee		28/02/2023

---

## **TABLE OF CONTENTS**

<b>1. INTRODUCTION .....</b>	<b>4</b>
<b>2. DIAMOND LIKE CARBON.....</b>	<b>5</b>
<b>3. ION BEAM DEPOSITION.....</b>	<b>8</b>
3.1. ION BEAM DEPOSITION SETUP AT INFN BARI.....	9
3.2. EXPERIMENTAL PRODEDURE AND DLC SAMPLES PRODUCED.....	10
<b>4. PULSED LASER DEPOSITION .....</b>	<b>13</b>
4.1. PULSED LASER DEPOSITION SETUP AT INFN LECCE .....	14
4.2. EXPERIMENTAL PRODEDURE AND DLC SAMPLES PRODUCED.....	15
<b>5. CHEMICAL WET ETCHING TEST .....</b>	<b>17</b>
<b>6. CONCLUSIONS AND OUTLOOK .....</b>	<b>19</b>
<b>7. REFERENCES .....</b>	<b>20</b>
<b>ANNEX: GLOSSARY.....</b>	<b>22</b>

## Executive summary

*This report details the studies done so far in scaling up Ion Beam Deposition (IBD) and Pulsed Laser Deposition (PLD) Diamond-like carbon (DLC) foils. The introduction outlines the current limitations in Magnetron sputtering created DLC foils, followed by a general introduction to DLC discussing properties and production techniques. The report continues discussing the IBD technique and setup at INFN Bari, the PLD technique at INFN Lecce and the DLC samples produced. The last part discusses the chemical wet etching procedure to fabricate an amplification foil with fine-patterned holes and the test in a prototype detector. The experience gained with well-controlled small-scale lab setups have allowed to gain valuable experience in sample preparation, deposition and qualification, and this know-how will be transferred to the operation of the new magnetron sputtering machine that is currently being commissioned at the CERN Micro-Pattern Technologies (MPT) workshop.*

## 1. INTRODUCTION

The present generation of Micro-Pattern Gaseous Detectors (MPGDs) are radiation hard detectors, capable of dealing with rates of several MHz/cm<sup>2</sup>, while exhibiting good spatial resolution ( $\leq 50 \mu\text{m}$ ) and modest time resolution of 5–10 ns, which satisfies the current generation of experiments (High Luminosity LHC (HL-LHC) upgrades of CMS and ATLAS) but is not sufficient for bunch crossing identification of fast timing systems necessary for background rejection in future collider experiments. The development of GEM foils with resistive electrodes allows for new detector concepts such as the fast-timing MPGD (FTM), which can achieve a time resolution improved by an order of magnitude while maintaining other MPGD properties such as rate capability and spatial resolution. MPGDs have proven their reliability, but can be further improved to minimize discharge propagation. Resistive electrodes for MPGDs will allow for a natural spark protection of the detectors, resulting in larger operational plateaus while these detectors will be able to stand much harsher background particle rates.

Diamond-Like Carbon (DLC) was pioneered in the MPGD collaboration as early as the 1990s for improvements to the Micro-Strip Gas Chamber (MSGC). In the last 10 years it has seen renewed interest by the development of large-size MicroMegas with resistive strips for the upgrade of the muon detection system of the ATLAS experiment (the New-Small-Wheel project) as well as the development of the micro-resistive well (uRWELL). The construction of these detectors does not require the patterning and etching of the DLC layer. However, for the development of resistive gas electron multipliers (GEMs) or fully resistive micro wells where all electrodes are resistive, the patterning and etching of the DLC layer becomes fundamental. This requires the production of more complicated base materials such as polyimide with a thin Cu layer that covers the resistive DLC layer.

The adherence of the DLC and Cu to the polyimide is of fundamental importance for the chemical wet etching process, since delamination leads to an increase of the hole diameter and bad coverage of the electrodes, resulting in low gain devices that cannot be used for particle detection. Furthermore, many different applications will benefit from the development of polyimide foils with resistive electrodes, e.g. fully resistive GEMs that are naturally spark protected to construct Triple-GEM detectors to be operated in the extremely harsh conditions of FCC-hh and the development of Gaseous Photomultipliers with very high gain, where spark-protection is a fundamental characteristic to achieve the high gains needed to detect single photoelectrons. Developing a new fundamental building block for the construction of MPGDs will open many possibilities for the development of new geometries, which we cannot imagine yet.

## 2. DIAMOND LIKE CARBON

Diamond-like carbon (DLC) is a metastable amorphous carbon film with carbon atoms bound in a mixture of  $sp^2$  and  $sp^3$  hybridizations [1, 2]. In the 1970s a series of experiments using carbon ion beams were pioneered by Aisenberg and Chabot to fabricate diamond films. They confirmed the formation of amorphous carbon films and named them diamond-like Carbon [3]. Fig. 1 illustrates the  $sp^2$  and  $sp^3$  hybridizations found in graphite and diamond, and the mixture of  $sp^2$  and  $sp^3$  found in diamond-like carbon.

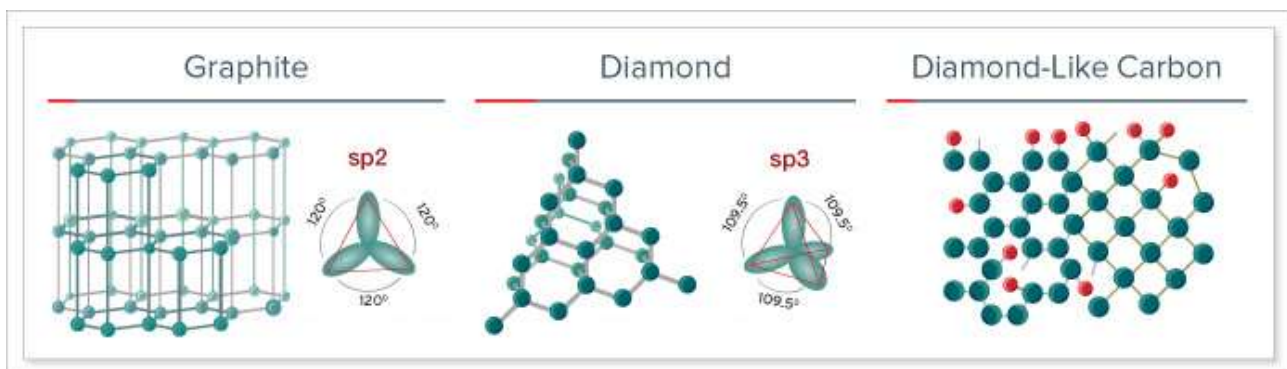


Fig. 1 Illustration of the  $sp^2$  and  $sp^3$  hybridizations of carbon found in graphite (pure  $sp^2$ ) and diamond (pure  $sp^3$ ). Diamond-like carbon is an amorphous material that consists of a mix of  $sp^2$  and  $sp^3$  hybridized carbon atoms [4].

DLC films have several attracting features such as: high mechanical hardness, high wear resistance, low friction coefficient, high resistivity, high chemical inertness, high gas barrier properties, high anti-burning properties, high biocompatibility, and the film is a wide band-gap semiconductor. DLC inherits most of its features from diamond, because of the presence of its strong directional  $\sigma$ -bonds between the  $sp^3$  orbitals. DLC films have wide-spread applications as coating, ranging from electric and electronic equipment, cutting tools, automotive parts, optical components, plastic bottle oxygen barrier films [5]. Hydrogen or nitrogen can be added to control the DLC properties such as resistivity, hardness, internal stress, and the stability of these properties in time.

Robertson et al. proposed a ternary phase diagram to characterize DLC films based on their content of  $sp^2$ ,  $sp^3$  and hydrogen [6], which is illustrated in Fig. 2. DLC films do not only consist of amorphous carbon ( $a$ -C) but can also contain hydrogenated alloys ( $a$ -C:H). Materials such as soot, and evaporated  $a$ -C have a disordered graphitic order and can be found on the lower left-hand corner which represent pure  $sp^2$  (graphite). Polyethylene  $(CH_2)_n$  and polyacetylene  $(CH)_n$  define the limits of the triangle on the right-hand corner, beyond which interconnecting C-C networks cannot form, and only molecules exist (no film) [1]. The third (upper) corner is pure  $sp^3$  (diamond).

DLC films can be categorized based on their  $sp^3$  to  $sp^2+sp^3$  ratio and H content: films with  $< 5\%$  hydrogen and  $sp^3/(sp^2+sp^3) > 50\%$  are named highly tetrahedral amorphous carbon ( $ta$ -C), while films with the same low hydrogen content but with  $sp^3/(sp^2+sp^3) < 50\%$  are named amorphous carbon ( $a$ -C). A higher concentration of hydrogen ( $< 50\%$ ) leads to DLC films labeled  $ta$ -C:H or  $a$ -C:H, depending on their  $sp^3/(sp^2+sp^3)$  ratio. Films where the hydrogen content is  $> 40\%$  and a linear carbon chain structure becomes dominant, are named Polymer-like carbon, and these films have typical lower hardness.

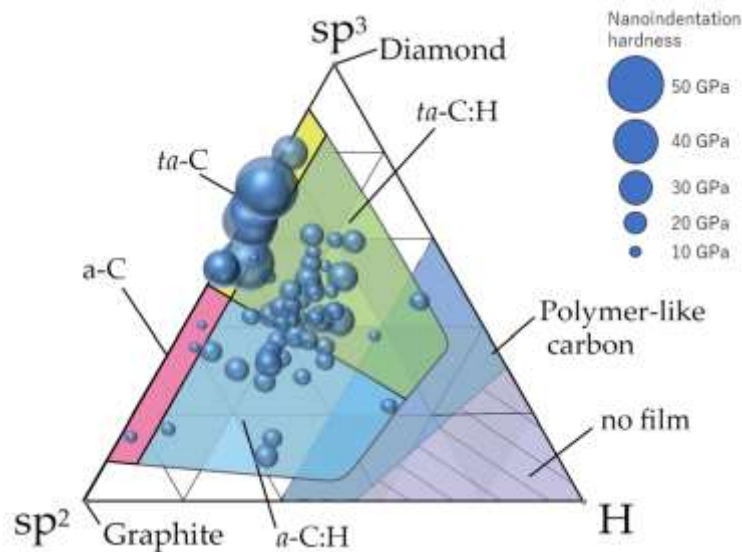


Fig. 2 Ternary phase diagram of various Diamond-like carbon structures that can be created with different  $sp^2/sp^3$  ratio and different hydrogen doping. Superimposed are the nanoindentation hardness of 74 DLC samples [5].

The growth mechanism of DLC films is understood in terms of subplantation (low energy sub-surface implantation) of incident ions [1]. The key property of DLC is its  $\sigma$  bond between  $sp^3$  orbitals, and the deposition process that promotes the formation of  $sp^3$  is ion bombardment with a ion energy around 100 eV [1].  $sp^2$  bonded graphite occupies 50% more volume than  $sp^3$  bonded diamond, making diamond more stable at high pressures. The role of the ion beam is to create a compressive stress in the film which promotes the formation of  $sp^3$  [1]. A low energy ion will not have enough energy to penetrate the surface (potential barrier of the surface), and will remain in the lowest energy state, which is  $sp^2$ . A higher energy ion will penetrate the surface and enter an interstitial state, resulting in an increase in the local density. It is assumed [1] that hybridizations will adapt to the local density, becoming more  $sp^3$  at high density.

The amorphous carbon films can be synthesized through chemical vapor deposition (CVD) techniques, such as plasma-enhanced CVD (PECVD), or through physical vapor deposition (PVD) techniques such as evaporation, ion plating and various sputtering and laser deposition techniques. Hydrogen-rich DLC ( $ta-C:H$  or  $a-C:H$ ) is typically produced through PECVD, while for the deposition of hydrogen free DLC mostly PVD techniques are used. In PECVD the plasma is created by a radiofrequency (RF) or a direct-current (DC) discharge between two electrodes in a volume filled with a hydrocarbon gas at low pressure. The deposition of hydrogen-free DLC requires a carbon source and a source to increase the energy of the carbon ions. The source can be an ionized hydrocarbon gas or a pure carbon target thermally evaporated, ion sputtered, or laser ablated [22]. The main technologies are briefly listed below [22]:

- *Direct ion beam*: electrostatically accelerated carbon ions created by sputtering (original method of Aisenberg and Chabot). A more controlled deposition is obtained through *Mass selected ion beam* deposition, where the beams are accelerated and passed through a magnetic filter, which selects ions with  $e/m$  ratio of  $C^+$  ions. Excellent control over the deposition is balanced by high cost and low deposition rate.
- *Arc discharge*: an electric discharge between a carbon cathode and anode creates a pure carbon plasma. The arc can be ignited by a laser (laser-arc discharge). This method is



characterized by high-purity and high deposition rates (100 nm/min), but with a broad (Maxwellian) energy distribution with a peak at ~30 eV, which can be increased by acceleration in an electric field. A purer carbon beam can be obtained with a magnetic filter (*Filtered arc discharge*).

- *Sputtering*: ions interacting on a carbon target create a beam of carbon ions directed to a substrate. This is the most common industrial process for deposition of DLC and is most often realized through DC or RF sputtering on a graphite electrode using an Argon plasma. Magnets are used to spiral electrons in the plasma to increase the deposition rate (*Magnetron sputtering*). Additional reactive gasses can be added (*Reactive sputtering*). Alternatively, a beam of Argon ions can be used to sputter from a graphite target to create a carbon ion beam (*Ion beam sputtering*, discussed more in detail in section 3).
- *Laser ablation*: A pure carbon plume is created by the interaction of an intense laser pulse on a carbon target (more details in section 4).
- *Ion assisted deposition* or *Ion plating*: where carbon ions from an evaporation source are bombarded by energetic noble gas ions. The momentum transfer is however low, limiting the sp<sup>3</sup> fraction obtainable by this technique.

Thin film properties are determined by the film-forming particles, important aspects are both their flux and their kinetic energy. Energy is lowest for evaporation (0.1-0.5 eV) and higher for magnetron sputtering and ion plating (1-100 eV). Pulsed laser deposition has both very low and very high energy particles (0.1-100 eV) while ion beam sputtering can have film-forming particles as high as several hundred eV [tutorial]. Fig. 3 (left) compares the typical energy range of the ions used in the growth of thin films through PVD techniques, while Fig. 3 (right) illustrates the growth rate of the films.

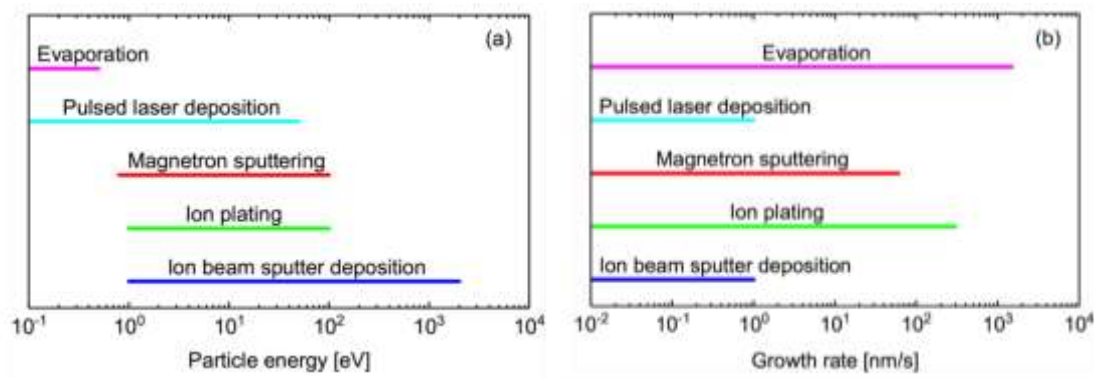


Fig. 3 Typical range of particle energy of the ions (left) and the growth rate (right) in some PVD techniques [12].

Fundamental for the application of DLC films in gaseous particle detectors is the good control of the surface resistivity, good uniformity and smooth surface, reduction of the internal stress and optimal adhesion to the polyimide foils. Further steps will require also long-term irradiation tests to verify the stability of the DLC film properties under endured operation in harsh radiation environments.

### 3. ION BEAM DEPOSITION

Ion Beam Deposition (IBD) also referred to as Ion Beam Sputtering (IBS) or Ion Beam Sputtering Deposition (IBSD) is a Physical Vapor Deposition (PVD) technique that produces very high-quality thin films with high precision [7]. The process is slow but allows for tight control over the film thickness and high control on the film quality. Two types of ion beam deposition can be distinguished [7]: ion beam deposition with beams of ions made of the material to be deposited [4,8] and ion beam sputtering deposition where the material comes from the sputtered target [9,10].

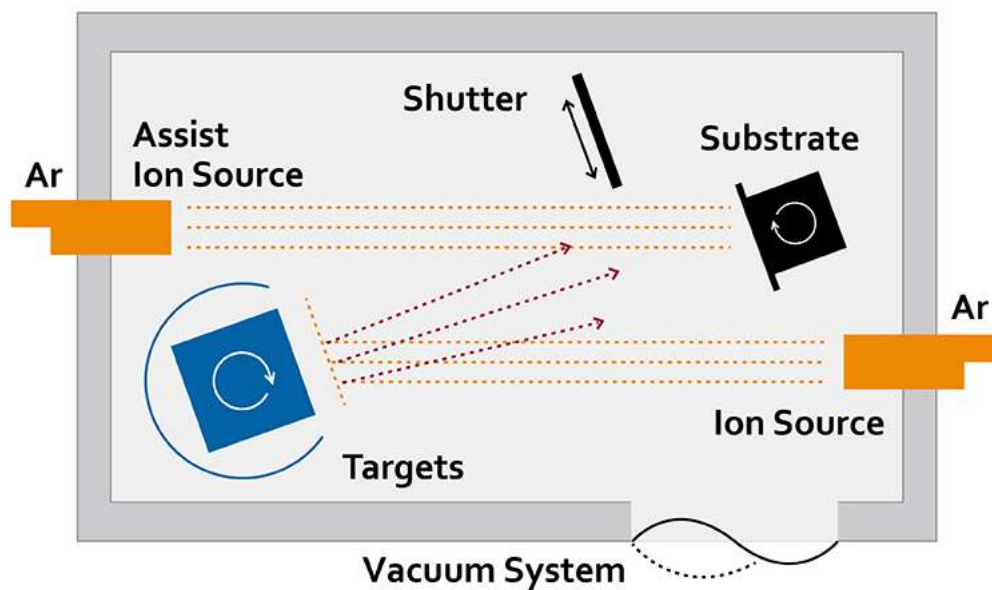


Fig. 4 Schematic view of an ion beam deposition setup with an assistant ion source [11].

Figure 4 illustrates the working principle of ion beam deposition: an ion source (typically ions of an inert gas, e.g. Argon) bombards a target, and the sputtered material is deposited onto a substrate. The setup may consist of a second ion source that is directed towards the substrate to aid the process. The ions released by assistance source compactify the film during the deposition, leading to a denser film with fewer defects. In ion beam deposition the bombarding ions are mono-energetic, which results in a highly collimated deposition process. IBS is among the most versatile and flexible techniques within the PVD portfolio, as it can grow very thin layers with good uniformity thanks to independent control of the sputtering ion energy and current [12]. In contrast to DC or RF sputtering, in IBS the substrate is not directly exposed to the gas discharge, that is localized in the ion beam sources. The low energy and high current assistance ion source can be used to direct ions of different gases towards the substrate. The assistance source is particularly useful to perform chemical or physical treatment of the substrate surface (e.g. cleaning, passivation of dangling bounds) before, during and after the sputter depositions. Reactive gases ( $O_2$ ,  $N_2$ ,  $H_2$ ) can be used during film growth to promote the formation of Oxides, Nitrides or Hydrogen bounds in the deposited film. The good control of the sputtering and assistance source parameters allows to obtain compounds with controlled stoichiometry (e.g. control over  $x \in \mathbb{R}$  in the deposition of a  $TiO_x$  film), by sputtering on a pure metal target. On the contrary, the same control can be obtained using hydrogen in assistance beam to reduce metal-oxides used as target material.



### 3.1. ION BEAM DEPOSITION SETUP AT INFN BARI

At INFN Bari and University of Bari, a custom-made vacuum chamber was equipped with two Kaufman ion sources [9] for sputtering and one auxiliary ion source for assistance. The ion beam setup consists further of two target holders that can be rotated 180 degrees such that in total 4 different materials can be sputtered on a substrate in the same run (i.e. without breaking the vacuum conditions). The targets are 10 cm diameter each, and they determine the size for uniform film growth on the substrate to about 10 cm<sup>2</sup>. The ion sources bombard the targets under an angle of 45 degrees, while the assistance ion source is focussed directly on the substrate at a lower angle. The substrate holder consists of a rotating plate that can be heated up to 900 °C. A quartz micro-balance near the substrate holder allows to control the film thickness during the growth. The setup is described in detail in [13] and is illustrated in Figure 5.

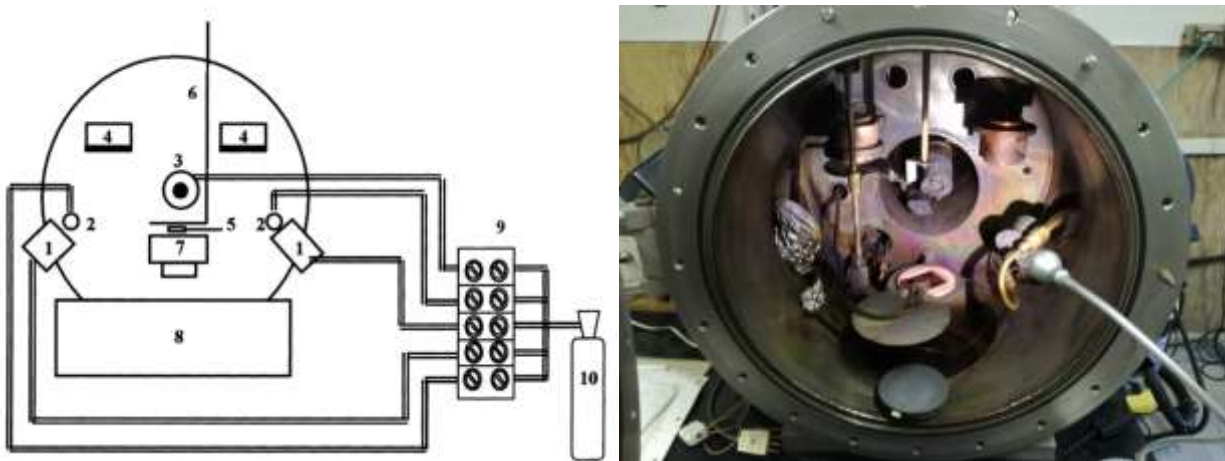


Fig. 5 Left: Schematic view of an ion beam deposition setup with an assistant ion source [3.3]. Right: Photograph of the same setup. Components: (1) Kaufman ion beam sources; (2) plasma bridge neutralizers; (3) assistance ion beam source; (4) rotatable targets; (5) quartz micro-balance; (6) shutter; (7) substrate holder; (8) turbomolecular pump; (9) gas flow control unit; (10) gas supply.

The ion beams that bombard the target are created inside double-grid sources. Electrons are thermionically emitted from a filament cathode, after which they are accelerated and made spiralling in an electrical and magnetic field. Inside the source the electrons impact neutral atoms (typically Argon), which results in the creation of ions. The ions are then focussed, extracted, and accelerated through appropriate biasing the double Frisch grids of the ion source. The HV biasing of the Frisch grid allows precise control over the ions kinetic energy that will bombard and liberate atoms from the target, e.g. a potential difference of 800 V will result in ions being emitted with a kinetic energy of 800 eV. The use of a double grid allows the creation of high energy ion beams and to focus the ions exactly in the grid openings. Ideally all ions are focussed in the holes, such as not to destroy the grid. Therefore the current of those beams needs to be kept at moderate levels, to take care of non-perfect focussing of the ion beam, which leads to a small fraction of the ions to collide with the second grid. This fraction is monitored in the setup by the current on the 2<sup>nd</sup> accelerator grid ( $I_{acc}$ ), which is to be kept as low as possible. The assistance ion beam is a high-current low-energy source, realized through a grid-less ion source, where ionization of the gas occurs outside the source itself, with electrons provided by a nearby electron source. The ionized atoms are then repelled by a positive potential set to the ring-shaped electrode of the ion source and directed to the substrate.

Typical operating parameters for the ion beam deposition are the following:

- Ion beam source:  $V_{beam} = 600\text{--}1200\text{ V}$ ;  $I_{beam}$  of 50–90 mA;
- Assistant ion source:  $V_{beam} = 50\text{--}150\text{ V}$ ;  $I_{beam}$  of 50–1200 mA.

### 3.2. EXPERIMENTAL PRODEDURE AND DLC SAMPLES PRODUCED

The recipe to produce high-quality DLC films with uniform resistivity was pioneered on tests performed in 2018-2019 [14] and a set of parameters were found to produce adherent DLC films with a surface resistivity of 100 ( $\pm 10$ ) MOhm/sq on Kapton foils and are listed in Table 1. The surface resistivity values are determined with 10% uncertainty and the reproducibility of the film resistivity was verified.

Tab. 1 Parameters for main and assistance ion beam sources for the deposition of a 100 MOhm/sq DLC film.

sample	Main ion source			Assistance ion source				DLC properties	
	$V_{beam}$	$I_{beam}$	Ar	$V_{beam}$	$I_{beam}$	Ar	H <sub>2</sub>	thickness	Resistivity
#1926	800V	50mA	2.5sccm	80V	50mA	2.0sccm	1.0sccm	50nm	100MOhm/sq
#1929	800V	50mA	2.5sccm	80V	70mA	2.1sccm	1.05sccm	50nm	115MOhm/sq

The adhesion of the DLC to the Kapton was verified through tests with scotch tape which are standard in the sector: no DLC could be removed and the DLC was found very well attached to the substrate. Measurements were performed over the timespan of a week and no change in the resistivity of the film was observed. The next step was to cover the DLC with a layer of copper such that the structure can be processed with the standard processes used for detector production: photolithography and chemical wet etching. Further tests were made in early 2020 [15] and the following procedure was found to give a Cu layer with good adherence to the DLC:

- Cleaning of the DLC surface: 10 minutes of assistance ion source (Ar ions, 150 eV, 1 A);
- Deposition of a 10 nm layer of Cr or Ti on top of the DLC film before the 100 nm Cu layer.

The results of the scotch test performed on the Cu top layer are shown in Fig. 6, as well as the result of a scratch test with horizontal and vertical cuts, where no Cu was removed after scotch test.



Fig. 6 Results of the scotch tape test on top of the final copper layer (50 nm). When copper is removed by the tape this indicates an insufficient adhesion, when instead no copper can be noticed on the yellow Kapton tape after the test the adhesion is good. Left: insufficient adhesion of Cu in a sample with 10 nm Aluminium interlayer (top) and a 10 nm Titanium interlayer (bottom). Middle: good adhesion of Cu obtained through cleaning of the DLC layer before the deposition of a 10 nm Titanium interlayer (top) or 10 nm Chromium interlayer (bottom). Right: results of a scratch test: no Cu was removed by the scotch tape test after vertical and horizontal cuts on the Cu top layer [15].

Although most Covid restrictions were brought back to moderate levels at the start of the AIDAInnova project in March 2021, the pandemic was far from over and work did not restart until late spring 2022. First objective was to reproduce the results obtained in 2018-2020 and to validate the recipe. First tests on  $6 \times 6 \text{ cm}^2$  samples were made and were tested for adhesion at the CERN Micro-Pattern Technologies (MPT) Workshop before proceeding eventually with the patterning and etching to make detector-ready amplification foils. The thickness of 100 nm of Cu was found to be too thin as the Cu layer oxidized and had to be cleaned before electroplating to  $7 \text{ }\mu\text{m}$ . Therefore, we scaled up the thickness of the Cu layer from 100 nm to 500 nm and it was decided to store and transport the samples in vacuum bags. The next step was the production of samples with size of  $10 \times 10 \text{ cm}^2$ , which is the maximum size for which uniform films can be made and is also the maximum size of substrates that can be inserted in the vacuum chamber. A new substrate holder was prepared at INFN Bari (Fig. 7).

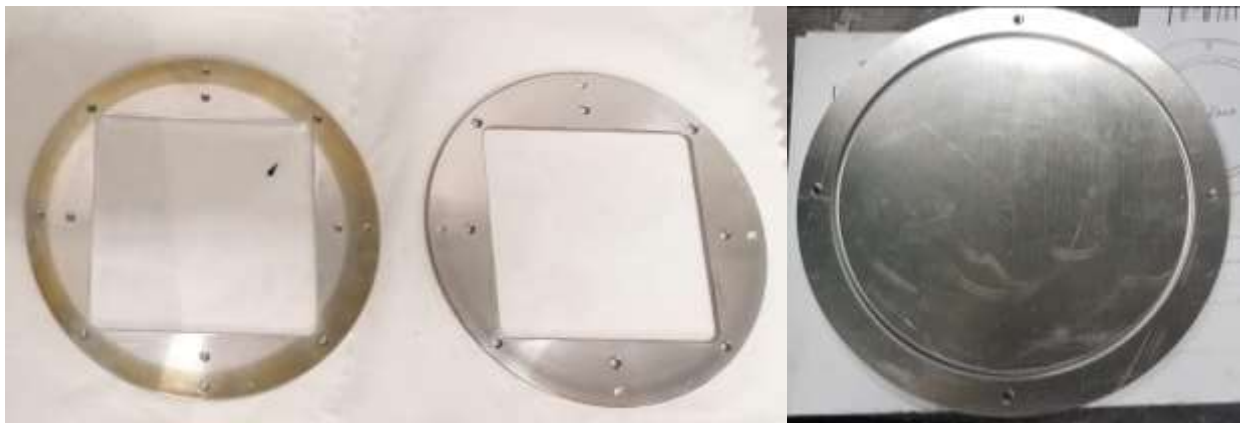


Fig. 7 Left: first  $10 \times 10 \text{ cm}^2$  substrate holder with hollow bottom. Right: second  $10 \times 10 \text{ cm}^2$  substrate holder with full aluminium backplate to ensure flatness during DLC deposition.

As substrate an Apical Kapton foil was first prepared in the lab with RCA standard cleaning steps (a standard set of wafer cleaning steps - Radio Corporation of America) [16], inserted in the substrate holder and mounted into the vacuum chamber. The vacuum chamber was pumped down to  $10^{-4} \text{ Pa}$  and the substrate was then cleaned with the assistance source for 5 minutes. The ion beam source sputtering on the first carbon target (pyrolytic carbon, purity 5N) was configured and operated for 2 hours together with the assistance source until a film with 50 nm was created (deposition rate 25 nm/h). As the deposition was interrupted (without breaking the vacuum), the DLC was first cleaned for 5 minutes with the assistance source, before continuing the deposition process with a Titanium interlayer of 10 nm (at  $\sim 100 \text{ nm/h}$ ). The film structure was finalised with a deposition of a 500 nm thick layer of copper, in a first step of 12' to create a 30 nm layer at approx. 150 nm/h and a second step of 2h22' to create the subsequent 470 nm, where the speed was increased to 200 nm/h. As the deposition of the Cu was interrupted and performed in two steps, before the final step an additional cleaning of the Cu was performed with the assistance ion source to avoid internal Cu delamination due to the presence of impurities trapped.

Tab. 2 Parameters for main and assistance ion beam sources for the deposition of a multi-layer DLC-Ti-Cu film

	step	Main ion source			Assistance ion source				Notes	
		$V_{beam}$	$I_{beam}$	Ar	$V_{beam}$	$I_{beam}$	Ar	H <sub>2</sub>	time	thickness
1	PI cleaning	-	-	-	150V	1A	5.1 sccm	4.0 sccm	300s	-
2	DLC layer	800V	50mA	2.5sccm	80V	50mA	7.3 sccm	2.0 sccm	7200s	50 nm
3	DLC cleaning	-	-	-	150V	1A	5.1 sccm	-	300s	-
4	Ti interlayer	1300V	35mA	2.5sccm	-	-	-	-	1260s	10 nm
5	Cu layer I	1000V	50mA	2.5sccm	-	-	-	-	720s	30 nm
6	Cu cleaning	-	-	-	150V	1A	5.1 sccm	-	300s	-
7	Cu layer II	1200V	60mA	2.5sccm	-	-	-	-	8520s	470nm

Steps 3 and 6 can be avoided by growing the layers in the same day without any interruption, as was done previously for samples with thinner DLC and copper layers. Comparison of Tab. 1 and Tab. 2 shows that a polyimide cleaning step was introduced as a first step to prepare the kapton surface for DLC deposition. In particular, the gas used for the assistance ion beam was a mixture of hydrogen and argon, and also the ion kinetic energy was increased (150 eV). This procedure has two goals:

1. Physical cleaning of the Kapton surface by high energy Ar ions.
2. Change in chemical surface properties by hydrogen ions.

In fact, the surface of polymers like kapton are generally hydrophobic, not only for water, but these properties can be extended to other materials likes metals or dielectrics. Plasma or ion treatments open the bounds of the polymers and increase as such the surface wettability [17].

A first 10×10 cm<sup>2</sup> sample was produced with the parameters indicated in Tab. 2. The film was however found to be bended at the end of the deposition process as the sample holder was hollow at the bottom. Therefore, a second sample holder was produced with a full aluminium backplate. Fig. 8 shows the vacuum sealer used in the laboratory to store and ship the samples to CERN (left) and the first 10×10 cm<sup>2</sup> sample produced. More samples are being produced this year, as the chemical etching steps (detailed in section 5) are elaborate, and the workshop would like to process multiple samples at the same time.



Fig. 8 Left: Vacuum equipment to prevent the top Cu layer from oxidation: vacuum sealer for domestic use and a first 6x6 cm<sup>2</sup> DLC-Cu deposition sealed in a vacuum bag. Right: first 10×10 cm<sup>2</sup> DLC-Cu deposition sealed in vacuum.



## 4. PULSED LASER DEPOSITION

Pulsed Laser Deposition (PLD) is a physical vapor deposition technique like IBD and both are bottom-up approaches. PLD differs from IBD in the way the species to be deposited in thin film form are created. This aspect generates films with different properties. In PLD, a pulsed high-energy laser beam, with emission generally in the ultraviolet (UV) range, is directed at a solid target formed by the material to be deposited as a thin film. When the laser pulse is absorbed by the target, the energy is first converted into electronic excitation and then into thermal, chemical, and mechanical energy resulting in the formation of a forwardly peaked plasma plume containing many energetic species including atoms, molecules, electrons, ions, clusters, as illustrated in Fig. 9. The energy of the ablated ions in the plume is few 10-100 eV. The energy distribution and composition of the ions is governed by the fluence (energy deposited by a laser pulse per unit surface) of the laser beam. The ablated elements are deposited on a substrate placed a few centimeters (2-10 cm) from the target. The ablation process can be carried out either in high vacuum (congruent ablation) or in the presence of a low-pressure reactive gas ( $10^{-2}$ - $10^2$  Pa) that promotes compound formation (reactive ablation). The high kinetic energy of the species and large instantaneous flux ( $\sim 10^{14}$ - $10^{15}$  ions per  $\text{cm}^2$  per pulse) are responsible of films with specific properties (high density) or showing metastable phases, that are generally not achievable with conventional techniques.

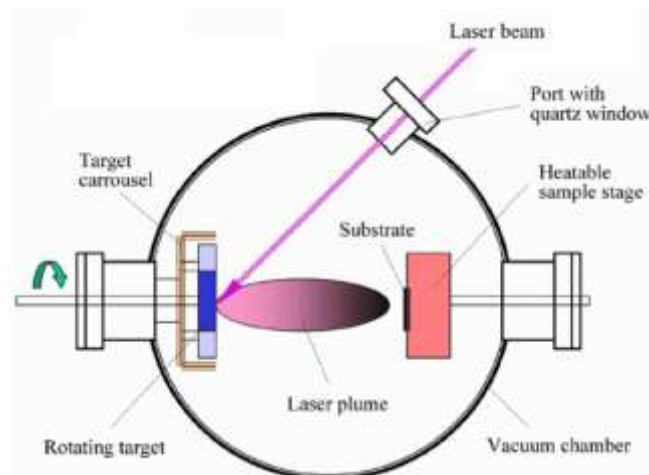


Fig. 9 Schematic view of a pulsed laser deposition setup, consisting of a vacuum chamber, a rotating target hit by a laser beam that creates a plasma plume directed towards to substrate that can eventually be heated up [18].

The main advantages of the laser ablation technique are:

- stoichiometric transfer of the material from target to substrate, under controlled conditions;
- good adhesion on different kind of substrates (even thermolabile substrates);
- lower substrate deposition temperature respect to other PVD techniques;
- deposition of multilayers in a single step;
- deposition on complex and patterned substrates;
- many independent deposition parameters;

The forward peaked plume has however an important disadvantage in the deposition of uniform thin films over a large area (more than a few  $\text{cm}^2$ ) and different strategies must be adopted to overcome this limit. However, PLD is an appealing alternative deposition technique for DLC films because of the high energy of the ablated species which is a fundamental prerequisite for the deposition of DLC

films. In fact, the formation of  $sp^3$  metastable bonds is driven by an energetic flux of impinging  $C^+$  ions (around  $\sim 100$  eV) yielding sub-plantation processes (i.e., shallow implantation where shallow means subsurface, within a few nanometers) with incorporation of the energetic C species that promote  $C(sp^2)$  to  $C(sp^3)$  transformation. The hyperthermal character of PLD also enables to obtain high fraction of  $C(sp^3)$  bonds at low growth temperatures, which is particularly appealing to deposit DLC films onto thermally sensitive substrates. Further, the possibility to have many independent deposition parameters for the film growth enables to have a fine control of the  $sp^3/sp^2$  ratio. In this respect the laser fluence plays a fundamental role in determining the film properties.

#### 4.1. PULSED LASER DEPOSITION SETUP AT INFN LECCE

At INFN Lecce and University of Salento two experimental set-ups for PLD depositions are present equipped with two different laser sources: a Nd:YAG laser and a KrF excimer laser. For DLC deposition the experimental set-up with a 248 nm KrF excimer laser (Lambda Physik LPX-305i) with 20 ns pulse length was used. The depositions have been carried out in a stainless-steel vacuum chamber evacuated down to a background pressure of  $\sim 10^{-5}$  Pa by a combined system of rotary and turbo-molecular pumps. The setup is shown in Fig. 10.



Fig. 10 PLD lab at INFN Lecce. Left: Eximer laser. Right: Vacuum vessel with (not visible) target and substrate holder.

For the deposition, the laser beam is focused on the target surface, a pyrolytic graphite target (5N purity = 99.999%) for DLC depositions, with a repetition rate of 10 Hz and with an angle of  $45^\circ$  with respect to the target normal. The laser beam scans on the graphite target along a XY-motorized spiral path to avoid forming craters due to repeated ablation of the same target area. Different kind of substrates ( $\langle 100 \rangle$  Si, silica and polyimide foils) can be placed in the substrate holder, parallel to the surface of the target, and at a target-to-substrate distance ( $d_{TS}$ ) of 5.5 cm.



## 4.2. EXPERIMENTAL PRODEDURE AND DLC SAMPLES PRODUCED

The substrate is carefully cleaned before being inserted in the substate holder: it is kept in an ultrasonic bath with acetone and isopropanol for 15 minutes at 60°C. About 7000 to 8000 laser pulses (12 - 15 minutes) are required to grow hydrogen-free DLC films with thickness in the range of 30 to 180 nm. To study the influence of the energy of the the ablated species in determining the  $sp^3/sp^2$  ratio and consequently the film electrical properties, the films have been deposited with different laser fluence values from 3.3 to 6.5 ( $\pm 0.3$ ) J/cm<sup>2</sup>. A focusing lens allowed to vary the spot area between 3 and 4 mm<sup>2</sup>. Under these conditions an unconventional V-shaped plasma plume was observed and studied [19]. Further, to obtain uniform films over a 2x2 cm<sup>2</sup> surface area different deposition geometries have been adopted. Qualitative information about the evolution of the formation of C(sp<sup>3</sup>)-bonds versus fluence was gained by non-destructive visible Raman spectroscopy. Structural and morphological analyses were performed by transmission electron microscopy (TEM), high resolution transmission electron microscopy (HRTEM) and selected area electron diffraction (SAD) patterns. Average sheet resistivity was measured by a 4-point probe system in air at room temperature [19]. The adhesion of DLC to the polyimide was found satisfactory (no removal of DLC with scotch tape test).

While the production of hydrogen-free DLC films with stable resistivity value of 100 MOhm/sq was demonstrated on 2x2 cm<sup>2</sup> surfaces [19], the technique, to be interesting for the development of small-scale detector prototypes needs to be scaled up, first to 5x5 cm<sup>2</sup>, and ultimately to 10x10 cm<sup>2</sup> areas. Another problem to be addressed was the subsequent deposition of copper on the DLC. Experience with IBD lead us to adopt immediately the procedure that all layers must be deposited without breaking the vacuum and the deposition of a chromium interlayer for the adhesion of Cu on DLC.



*Fig. 11 The result of the electroplating of a 7  $\mu$ m Cu layer on top of three 5x5 cm<sup>2</sup> PLD made Cu-Cr-DLC-Polyimide foils. One can clearly observe the delamination of the electroplated Cu layer after drying of the sample.*

Films up to  $5 \times 5 \text{ cm}^2$  were deposited successfully on  $7 \times 7 \text{ cm}^2$  polyimide foils (the minimum size required for performing chemical wet etching tests). To enhance the DLC to Kapton adhesion, the Kapton foils were first treated with an Argon plasma before the PLD process. Building upon the know-how developed with the IBD DLC deposition, multiple targets were installed in the PLD vacuum chamber to subsequently deposit a 10 nm film of Chromium followed by a 100 nm film of copper, without removing the sample from the vacuum chamber. The copper demonstrated good adhesion as we were not able to remove it with the scotch test. The manufactured films were then sent to CERN's MPT workshop to grow the Cu layer up to a thickness of  $7 \text{ }\mu\text{m}$ , necessary for the subsequent photolithography and wet-etching processes. The result of the Cu electroplating on three  $5 \times 5 \text{ cm}^2$  samples is shown in Figure 11. The Cu layer was found however not well adherent to the DLC and delaminated during the drying step after electroplating. The origin was traced back to the oxidation of the original 100 nm copper layer covering the DLC. In a subsequent test we tried to remove the thin Cu-oxide layer by polishing, but this was found to remove all Cu and reveal the DLC. Therefore, it was decided to increase the thickness of the final Cu layer to 500 nm and to ship the samples in vacuum to limit to a minimum the copper oxidation. Fig. 12 shows a DLC film with estimated resistivity of 100 MOhm/sq (left) and the final sample after deposition of a 500 nm Cu layer (right). This solution lead finally to a high-quality electroplating of a  $7 \text{ }\mu\text{m}$  thick copper layer and on this final sample the various steps of the chemical wet etching procedure could be applied and are discussed in the next section.

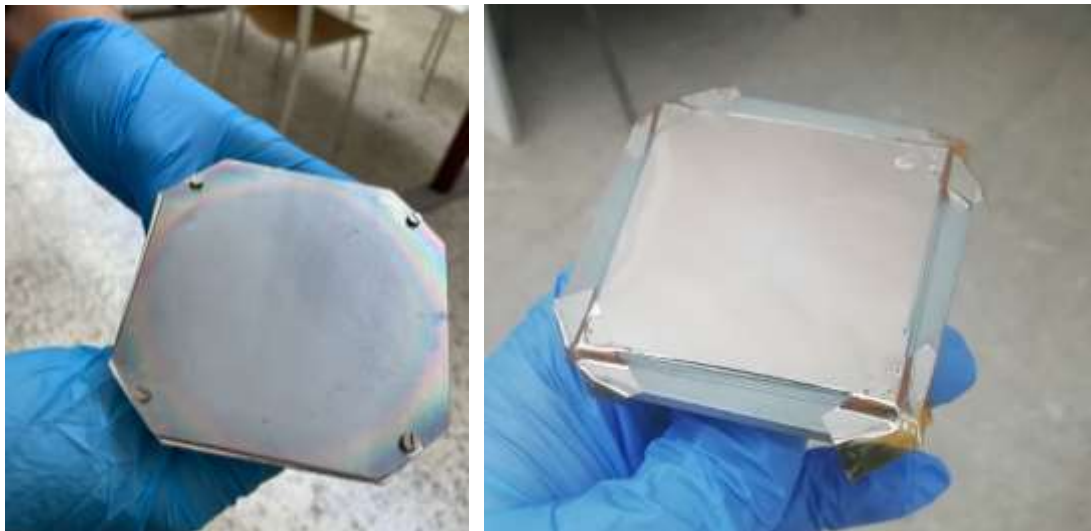


*Fig. 12 Left: DLC deposited on a  $7 \times 7 \text{ cm}^2$  polyimide foil. The DLC is deposited uniformly in a circle of 5 cm diameter. Non-uniformity at the borders can be observed visually (interference fringes). Right: final  $5 \times 5 \text{ cm}^2$  DLC film now covered by a 500 nm Cu layer.*

## 5. CHEMICAL WET ETCHING TEST

The adhesion of the Cu cover layer on top of the DLC film for the 5×5 cm<sup>2</sup> DLC foil made through PLD deposition (see section 4) was tested in the MPT workshop through a standard scotch test. The last sample produced finally passed the test and the foil was etched to a detector-grade amplification foil by the procedure outlined below. First the Cu layer on top of the DLC was grown through electroplating to a total thickness of 8 μm.

DLC is a very hard material, and no techniques have been perfected to allow patterning and etching starting from the side of the polyimide foil covered with DLC, the etching must be performed starting at the bottom, Cu-only side. The etching procedure of the DLC foils for the FTM is detailed in [20], in this paragraph a summary is given. The first step in the etching procedure is a thorough cleaning using sandblasting to remove impurities and subsequent drying in an oven. Thereafter a photoresistive layer is laminated on both sides, a mask is applied to the Cu-only side and the mask is developed with UV-light. The hole pattern is now transferred to the foil and the resist protects the Cu-layer that should not be etched. The uncovered Cu area is dissolved in FeCl<sub>3</sub>, and the 10 nm Cr layer used for Cu adhesion to the polyimide was removed with a warm permanganate solution. Now the resist is removed, and the Cu layer can serve as a mask for the etching of the polyimide. The polyimide is etched in a solution of ethylenediamine and potassium hydroxide. The diameter of the holes is proportional to the etching time but depends also on the exact concentration of the chemical baths, which vary in time. Therefore, the etching time is calibrated for each etching individually by taking some sample material from the side and performing tests. The last steps consist of removal of the Cu layer that has served up to now as protection layer of the DLC and sand blasting of the foil to remove the thin DLC layer that is covering the holes. Fig. 13 (left) shows the finished amplification foil. A Cu ring encircles the hole patterned DLC layer in the center and serves for the polarization of the foil. Fig 13 (right) shows a microscope view of the etched holes: the hexagonal pattern is regular, and most holes have the desired diameter of 50 μm, etching imperfections are however visible, with several holes having non-circular shapes.

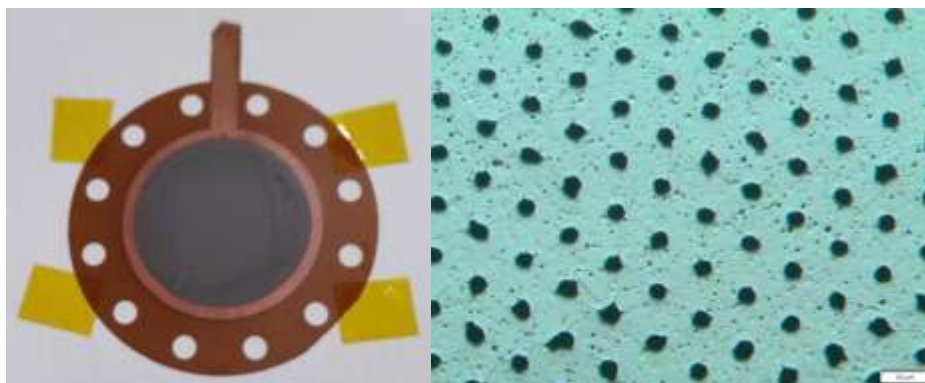


Fig. 13 Left: DLC coated amplification foil made in the CERN MPT workshop. A Cu ring with diameter of 2 mm encircles a 2 cm diameter DLC coated polyimide film that is patterned with a hexagonal structure of 70 μm diameter holes spaced 140 μm apart. Right: detail of the patterned area. Visible are slight imperfections in the DLC foil and because of the non-fully mastered etching with DLC coatings, one can observe some holes with larger diameter of non-circular shape.

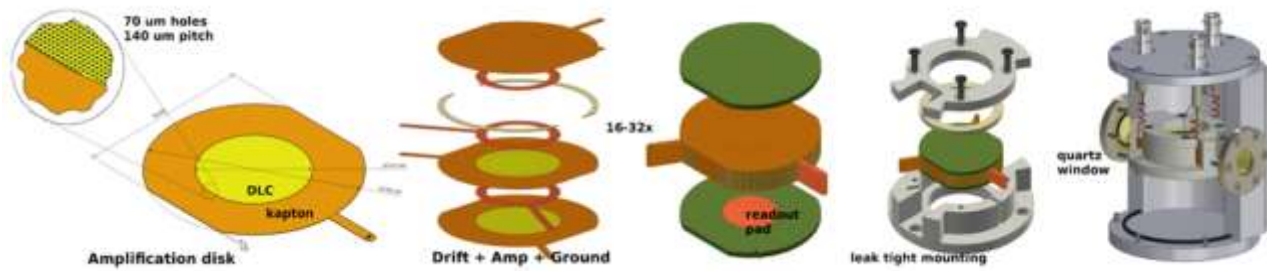


Fig. 14 Overview of the small FTM prototype. It can host a stack of 32 layers with 250  $\mu\text{m}$  thickness. A single layer consists of non-patterned DLC foils as ground and cathode electrodes and a patterned DLC foil for amplification. For the tests described in the report a single layer was used with a drift gap of 1.2 cm. The FTM has 2 quartz windows to allow the laser beam to be focused inside the gas gap.

The PLC-DLC foil was inserted in the Fast Timing MPGD prototype (see Fig. 14) with quartz window and the detector was filled with Ar : CO<sub>2</sub> : iC<sub>4</sub>H<sub>10</sub> 93:5:2 gas mixture. A potential difference of 450 V between top and bottom of the amplification structure was applied, with a drift field of 3 kV. The laser setup consists of a Nd:YAG pulsed laser with 266 nm wavelength (CryLaS 266-50) with a controllable pulse energy of 10 – 51  $\mu\text{J}$  and pulse duration of 0.9 – 1.3 ns and waist of 400  $\mu\text{m}$  was used to ionize the gas inside the FTM through two-photon interactions on impurity atoms in the gas (benzene, toluene, ...) [21]. The laser beam is focused to a spot of  $\sim 25 \mu\text{m}$  to create a narrow point of primary ionization. The primary electrons then drift and are amplified inside the foil that was kept at 450 V. Fig. 15 illustrates the signals induced in the readout. A clear signal is amplified with the Cividec C2-HV 40dB 2GHz broadband amplifier before being acquired by an oscilloscope. The amplified signals have an amplitude of about 150 mV and represent a charge of  $\sim 1.75 \text{ fC}$ . This setup can be used to make a gain curve for the amplification foil, which will be done soon. Full characterization of the foil is ongoing.

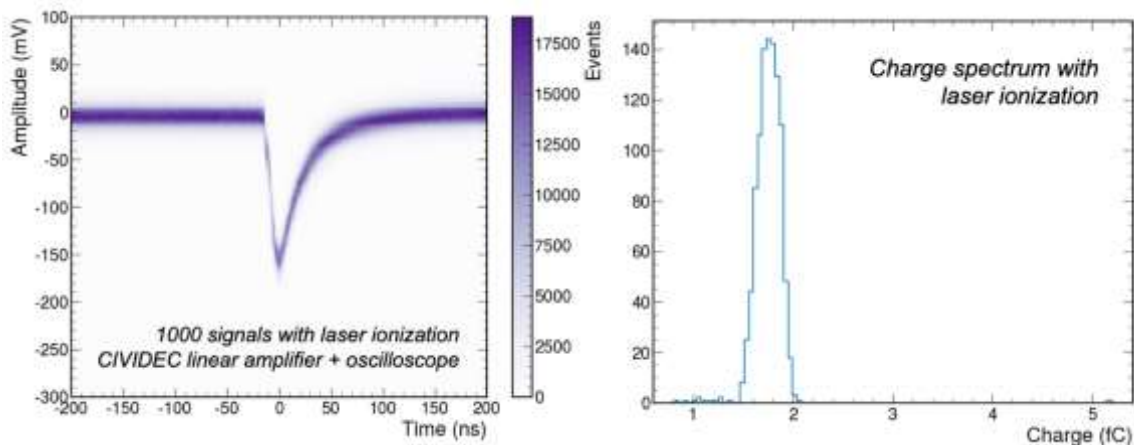


Fig. 15 Left: Average of 1000 signals picked up by the readout electrode of the signal pulse induced by the laser ionization in the detector. The signal was amplified with a 40 dB broadband (2 GHz) current amplifier and acquired on an oscilloscope. Right: charge spectrum of the same signal obtained by integrating the signal, an average signal of 150 mV and 1.75 fC was observed.



## 6. CONCLUSIONS AND OUTLOOK

This report summarizes the work on the production of detector-grade polyimide foils with thin DLC films through the upscaling of laboratory techniques (Ion Beam Deposition – IBD, and Pulsed Laser Deposition - PLD) to larger area. The current state-of-the-art large size DLC foils produced through magnetron sputtering are not yet of good quality such to allow the use of lithographic techniques, required for the fabrication of resistive GEMs or fully resistive micro-WELL amplification structures. The DLC films produced through IBD and PLD have demonstrated controlled uniform resistivity and good adherence [14,19]. Within the AIDAinnova project, we have investigated the subsequent deposition of a copper layer, which must have a very high adherence, to allow photolithography. The advantages of IBD and PLD is the creation of very dense and adherent films, yet at much lower deposition speeds and covering a reduced surface area. A recipe based on substrate cleaning, the use of a 10 nm titanium or chromium interlayer and the increase of Cu thickness to 500 nm lead to detector-grade Cu-covered DLC film depositions on polyimide. The first foil (5×5 cm<sup>2</sup>) was used to create an amplifying structure that was found to have reasonably good performance. Through IBS two foils of 10×10 cm<sup>2</sup> have been produced already, while for PLD we are investigating how to increase to a similar size. Further etching tests on these foils are required to investigate the quality of the foils after etching and to verify whether the final product is of higher quality with respect to the previously produced industrial DLC foils.

The increasing use of DLC in the fabrication of resistive MPGDs in 2010-2020, has led to the organization of a topical workshop on DLC by the RD51 collaboration [23] in February 2020, where the acquisition of a DLC magnetron sputtering machine for the CERN MPT workshop was proposed. The machine, financed by CERN and INFN, was delivered in October 2022 and is currently being commissioned [24, 25]. This industrial machine can deposit thin films on polyimide foils of a size of 60 cm × 170 cm. Within this context we would like to apply the expertise gained through the IBD and PLD deposited foils to use the machine to produce DLC films with high density and good adherence, and to obtain multilayer structures (DLC – Chromium – Copper) with good adherence. The machine settings should be optimized to obtain DLC films with highest density. It would be interesting to verify the location of the DLC films on the ternary phase diagram (i.e. hydrogen content and sp<sup>3</sup> to sp<sup>2</sup>+sp<sup>3</sup> ratio). It will be as well of interest to verify the plasma treatment to clean the base polyimide foil before deposition and to investigate the addition of hydrogen on the quality of the DLC (passivation of dangling bonds) in order to test the adhesion of the various layers.

---

## 7. REFERENCES

- [1] Robertson J. (2002) Diamond-like amorphous carbon, *Materials Science and Engineering: R: Reports* 37 4-6 129-281, [https://doi.org/10.1016/S0927-796X\(02\)00005-0](https://doi.org/10.1016/S0927-796X(02)00005-0).
- [2] Ferrari A.C., Robertson J., (2000) Interpretation of Raman spectra of disordered and amorphous carbon, *Physical Review B* 61(20), 14095-14107. <https://doi.org/10.1103/PhysRevB.61.14095>
- [3] PVD Advanced Technologies. DLC Coatings [online], Available from: <http://www.pvdadvancedtech.com/dlc/> [Accessed 17/02/2023].
- [4] Aisenberg S. and Chabot R.W. (1971) Ion-Beam Deposition of Thin Films of Diamondlike Carbon, *Journal of Applied Physics* 42, 2953, <https://doi.org/10.1063/1.1660654>.
- [5] Ohtake N. *et al.* (2021) Properties and Classification of Diamond-Like Carbon films, *Materials* 14(2) 315, <https://doi.org/10.3390/ma1420315>
- [6] Robertson J. *et al.* (1994) Highly tetrahedral, diamond-like amorphous hydrogenated carbon prepared from a plasma beam source, *Applied Physics Letters*, 64, 2797–2799, <https://doi.org/10.1063/1.111428>.
- [7] Vossen J.L. and Kern W. (1978) *Thin Film Processes*, New York, Academic Press, ISBN 978-0127282503
- [8] Aisenberg S. and Chabot R.W. (1973) Physics of Ion Plating and Ion Beam Deposition, *Journal of Vacuum Science and Technology* 10, 104, <https://doi.org/10.1116/1.1317915>.
- [9] Harper J.M.E., Cuomo J.J. and Kaufman H.R. (1982) Technology and applications of broad-beam ion sources used in sputtering. Part I. Ion source technology, *Journal of Vacuum Science and Technology* 21, 725, <https://doi.org/10.1116/1.571819>.
- [10] Harper J.M.E., Cuomo J.J. and Kaufman H.R. (1982) Technology and applications of broad-beam ion sources used in sputtering. Part II. Applications, *Journal of Vacuum Science and Technology* 21, 737, <https://doi.org/10.1116/1.571820>.
- [11] Denton Vacuum. *What is Ion Beam Deposition?* [online], Available from: <https://www.dentonvacuum.com/what-is-ion-beam-deposition/> [Accessed 9/02/2023].
- [12] Bundesmann C, Neumann, H. (2018) Tutorial: The systematics of ion beam sputtering for deposition of thin films with tailored properties, *Journal of Applied Physics* 124, 231102, <https://doi.org/10.1063/1.5054046>.
- [13] Valentini, A *et al.* (2005) Ion-beam sputtering deposition of CsI thin films, *Applied Physics A* 80, 1789-1791, <https://doi.org/10.1007/s00339-004-3097-9>.



- 
- [14] Verwilligen P, Valentini, A, Caricato AP, *et al.* (2020) Diamond-Like Carbon for the Fast Timing MPGD, *Journal of Physics: Conference Series 1498 012015*, <https://doi.org/10.1088/1742-6596/1498/1/0122015>.
- [15] Valentini, A. (2020) Report on DLC Applications, RD51 Collaboration, RD51-NOTE-2020-006, 13 pages. <https://espace.cern.ch/test-RD51/RD51%20internal%20notes>
- [16] Kern, W. (1990) The evolution of Silicon Wafer Cleaning Technology, *Journal of The Electrochemical Society 137 1887*, <https://doi.org/0.1149/1.2086825>.
- [17] Siy Salapare III H. et al. (2009) The Porosity and Wettability Properties of Hydrogen Ion Treated Poly(Tetrafluoroethylene), in book: Contact Angle, Wettability and Adhesion (pp.207-216) 1<sup>st</sup> Edition, Chapter: 13, Leiden, Koninklijke Brill NV, ISBN 9789004169326. <https://doi.org/10.1163/ej.9789004169326.i-400.89>.
- [18] Robert Eason, Pulsed Laser Deposition of Thin Films: Applications-Led Growth of Functional Materials, John Wiley & Sons, Inc. (2007) ISBN:9780471447092 <https://doi.org/10.1002/0470052120>.
- [19] Caricato A.P. *et al.* (2022) Tailoring sheet resistance through laser fluence and study of the critical impact of a V-shaped plasma plume on the properties of PLD-deposited DLC films for micro-pattern gaseous detector applications, *Diamond & Related Materials 124 108909*, <https://doi.org/10.1016/j.diamond.2022.108909>.
- [20] Roskas C. (2021) The CMS GEM upgrade and development of Fast Timing Micro-Pattern Gaseous Detectors, PhD Thesis, Ghent University, 204p.
- [21] Pellicchia A., Ranieri A., and Verwilligen P. (2020) A UV laser test bench for micro-pattern gaseous detectors, *Journal of Instrumentation 15 04 C04011*, <https://doi.org/10.1088/1748-0221/15/04/C04011>.
- [22] Lifshitz, Y. (1999) Diamond-like carbon – present status, *Diamond and Related Materials 8 1659-1676*, [https://doi.org/10.1016/S0925-9635\(99\)00087-4](https://doi.org/10.1016/S0925-9635(99)00087-4).
- [23] RD51 collaboration (2021) RD51 DLC workshop report, RD51-NOTE-2021-002, 12 pages, <https://espace.cern.ch/test-RD51/RD51%20internal%20notes>.
- [24] De Oliveira, R. (2022) The Micro-Pattern Technologies Workshop at CERN, MPGD 2022 Conference, Rehovot, Israel, 12/12/2022, <https://indico.cern.ch/event/1219224>.
- [25] De Oliveira, R. (2023) The use of Micro-Pattern Technologies in Micro-Pattern Gaseous Detectors, CERN EP Seminars and Colloquia, 13/01/2023, <https://indico.cern.ch/event/1233427/>.

---

## **ANNEX: GLOSSARY**

<b>Acronym</b>	<b>Definition</b>
DLC	Diamond-Like Carbon
IBD, IBS, IBSD	Ion Beam Deposition, Ion Beam Sputtering, Ion Beam Sputtering Deposition
PLD	Pulsed Laser Deposition
RCA	Radio Corporation of America